Title

The Structure of the Periplasmic Sensor Domain of the Histidine Kinase CusS Shows Unusual Metal Ion Coordination at the Dimeric Interface

Journal

Biochemistry, 55(37)

ISSN

0006-2960

Authors

Affandi, Trisiani
Issaian, Aaron V
McEvoy, Megan M

Publication Date

2016-09-20

DOI

10.1021/acs.biochem.6b00707

Peer reviewed

Published in final edited form as:

Biochemistry. 2016 September 20; 55(37): 5296–5306. doi:10.1021/acs.biochem.6b00707.

The Structure of the Periplasmic Sensor Domain of the Histidine Kinase CusS Shows Unusual Metal Ion Coordination at the Dimeric Interface

Trisiani Affandi[1], **Aaron V. Issaian**[1,†], and **Megan M. McEvoy**[1,*]

[1]Department of Chemistry and Biochemistry, University of Arizona, Tucson, AZ 85721

Abstract

In bacteria, two-component systems act as signaling systems to respond to environmental stimuli. Two-component systems generally consist of a sensor histidine kinase and a response regulator, which work together through histidyl-aspartyl phospho-relay to result in gene regulation. One of the two-component systems in *Escherichia coli*, CusS-CusR, is known to induce expression of *cusCFBA* genes under increased periplasmic Cu(I) and Ag(I) concentrations to help maintain metal ion homeostasis. CusS is a membrane-associated histidine kinase with a periplasmic sensor domain connected to the cytoplasmic ATP-binding and catalytic domains through two transmembrane helices. The mechanism of how CusS senses increasing metal ion concentrations and activates CusR is not yet known. Here, we present the crystal structure of the Ag(I)-bound periplasmic sensor domain of CusS at a resolution of 2.15 Å. The structure reveals that CusS forms a homodimer with four Ag(I) binding sites per dimeric complex. Two symmetric metal binding sites are found at the dimeric interface, which are each formed by two histidines and one phenylalanine with an unusual cation-π interaction. The other metal ion binding sites are in a non-conserved region within each monomer. Functional analyses of CusS variants with mutations in the metal sites suggest that the metal ion binding site at the dimer interface is more important for function. The structural and functional data provide support for a model in which metal-induced dimerization results in increases in kinase activity in the cytoplasmic domains of CusS.

Copper is an essential metal element for most organisms because it acts as a cofactor in numerous biological processes[1]. However, only a small amount of intracellular copper is needed and excess amounts can be toxic even at low concentrations, in part due to its redox

*Corresponding Author: mcevoy@microbio.ucla.edu; Mailing: 611 Charles E. Young Drive East, Los Angeles, CA 90095-1570; Telephone: +1 (310) 206-5062, FAX +1 (310) 206-5365.

†**Present Addresses:** A.V.I.'s present address: Structural Biology and Chemistry, University of Colorado at the Anschutz Medical Campus, Aurora, CO, 80045.

*M.M.M.'s present address: Department of Microbiology, Immunology, and Molecular Genetics, University of California, Los Angeles, CA 90095.

Accession Code. The structure described here has been deposited as PDB entry 5KU5.

Author Contributions

The manuscript was written through contributions of all authors. All authors have given approval to the final version of the manuscript.

The authors declare no competing financial interest.

Supporting Information. Figure S1, electron density map of the $CusS_{(39\text{-}187)}$ metal binding sites; Figure S2, Western blot analysis of full length CusS wild type and mutants expressed from pET21b(+) plasmids; Table S1, bacterial strains and plasmids; Table S2, conversion between score and % cell survival. This material is available free of charge via the internet at http://pubs.acs.org.

properties[2, 3]. While silver is not required for any biological processes, it shares similar chemical and ligand binding properties with Cu(I), and it is also highly toxic at even lower concentrations[4]. Therefore, organisms have developed homeostatic mechanisms to tightly regulate copper and silver acquisition, sequestration, and efflux in order to protect the intracellular environment.

Bacteria live in changing environments and thus need systems that can respond to variations in external conditions. In bacteria, two-component systems are the major systems of signal transduction that help bacteria sense, respond, and adapt to chemical, physical and nutritional stimuli such as ions, pH, oxygen pressure, redox state, sugars and amino acids[5, 6]. A canonical two-component system consists of a sensor histidine kinase and a response regulator that work together through histidyl-aspartyl phosphorelay to respond to environmental conditions with changes in gene transcription. Many histidine kinases are homodimeric transmembrane proteins that consist of a variable periplasmic sensor domain flanked by two transmembrane α-helices which span the cytoplasmic membrane. The transmembrane helices in histidine kinases are expected to form dimeric four-helix bundles, similar to that observed in the sensory rhodopsin II in complex with its transducer[7]. The conserved kinase core is located in the cytoplasm. The classic signal transduction pathway of a histidine kinase-response regulator pair involves environmental stimuli detection by the periplasmic sensor domain of the histidine kinase and direct or indirect signaling to the cytoplasmic kinase domain. ATP-dependent auto-phosphorylation occurs at a conserved His residue in the kinase core. The phosphoryl group is then transferred from the histidine kinase to a conserved Asp residue on the N-terminal receiver domain of the response regulator, which in turn activates the C-terminal effector domain to mediate an adaptive response. The phosphorylated response regulator activates transcription of genes that respond to the environmental stimulus [5, 8].

In the Gram-negative bacterium *Escherichia coli* (*E. coli*), one of the cognate histidine kinase-response regulator pairs is CusS-CusR, which is the regulatory system for the expression of the *cusCFBA* genes in response to the accumulation of periplasmic Cu(I) or Ag(I). CusS is a canonical transmembrane histidine kinase with a periplasmic sensor domain, two transmembrane α-helices, and three domains in the cytoplasm: a “histidine kinase, adenylyl cyclases, methyl accepting proteins, phosphatases” (HAMP) domain, a dimerization and histidine phosphotransfer (DHp) domain, and a kinase core[5]. Previous studies have shown that the *cusS* gene is required for Cu(I)/Ag(I) resistance in *E. coli*; a cell strain with a *cusS* gene deletion has increased Cu(I)/Ag(I) sensitivity and decreased expression of the *cusC* gene[9]. The periplasmic domain of CusS consists of residues 39-187 and is approximately 17 kDa[10]. Biochemical studies have shown that $CusS_{(39\text{-}187)}$ binds Ag(I) ions and that the presence of Ag(I) enhances dimerization of $CusS_{(39\text{-}187)}$[11]. However, since no structures have been previously determined for a sensor domain responsive to Cu(I) or Ag(I), it is unclear how metal binding occurs and the relationship with dimerization. How the signal is transduced to the cytoplasmic kinase core is still unknown.

In this study we present the crystal structure of the Ag(I)-bound periplasmic sensor domain of *E. coli* CusS (Ag(I)-$CusS_{(39\text{-}187)}$) solved at a resolution of 2.15 Å. Mutagenesis combined with *in vivo* complementation assays were performed to investigate the functional

significance of metal ion binding. This work provides the framework for understanding the molecular role of CusS in Cu(I)/Ag(I) resistance and the mechanism of CusS signal transduction in *E. coli*.

MATERIALS AND METHODS

Protein purification and crystallization of Ag(I)-CusS$_{(39-187)}$

The pTXB3-CusS$_{(39-187)}$ plasmid was used for expression of CusS$_{(39-187)}$[11]. Apo CusS$_{(39-187)}$ and silver loaded CusS$_{(39-187)}$ (Ag(I)-CusS$_{(39-187)}$) were prepared as previously described[11]. Ag(I)-CusS$_{(39-187)}$ in 25 mM MES pH 6.0 buffer was concentrated to 7–8 mg/mL for crystallization. Initial crystallization of Ag(I)-CusS$_{(39-187)}$ was performed with commercially-available Index HT screening solutions (Hampton Research). Droplets consisting of 0.2 μL protein solution and 0.2 μL of each precipitant solution were mixed in sitting drops in a 96-well plate using a PHOENIX protein crystallization robot (Art Robbins Instruments). Clusters of rod-shaped crystals of CusS$_{(39-187)}$ formed after one week in a precipitant solution containing 100 mM Tris-HCl pH 8.5, 200 mM ammonium acetate, and 25% PEG-3350 at 4°C. The crystallization conditions were further optimized in the initial precipitant solution with varying PEG-3350 percentages and protein:precipitant ratios using sitting-drop vapor-diffusion at 4°C. Clusters of crystals were observed in all drops containing 100 mM Tris-HCl pH 8.5, 200 mM ammonium acetate, and 25% PEG-3350 with 1:2 protein:precipitant ratio. Diffraction quality protein crystals were obtained by equilibrating droplets against 1 mL precipitant solution using the sitting-drop vapor-diffusion method at 4°C. Crystals were flash frozen in liquid nitrogen.

Data collection, structure determination, and refinement

X-ray diffraction data for Ag(I)-CusS$_{(39-187)}$ were collected on the Stanford Synchrotron Radiation Lightsource (SSRL) beamline 7-1 at T=100 K and λ=1.494 Å. The diffraction data sets were processed and scaled with CrystalClear. The initial phases were obtained by the single anomalous diffraction (SAD) method using AutoSol Wizard. Initial model building was performed using AutoBuild Wizard (Phenix). Further model building and refinement were performed using COOT and REFMAC5. Data measurement, phasing, and refinement statistics are given in Table 1.

The structure of *E. coli* Ag(I)-CusS$_{(39-187)}$ was determined initially at a resolution of 2.80 Å using the SAD data collected at the higher wavelength (1.494 Å) from a single frozen crystal of Ag(I)-CusS$_{(39-187)}$ in space group $P22_12_1$ (Table 1). The model was then refined to 2.15 Å resolution against the data collected at a lower wavelength (1.036 Å). The R_{work} and R_{free} are 19.27 and 25.67%, respectively, and show good stereochemistry (Table 1). The asymmetric unit contains four CusS$_{(39-187)}$ molecules (referred to as chain A–D) and eight Ag(I) ions. Within the asymmetric unit, chain A and B form a dimer with four Ag(I) binding sites and chain C and D form another dimer with the other four Ag(I) binding sites. The two dimers in the asymmetric unit were related by non-crystallographic two-fold axes.

Residues 39-185 including the N-terminal Met were ordered in chain A. Chain B includes residues 39-184. Chain C includes residues 39-182 and has the poorest electron density in

which loop residues 122-125 were built in manually. Chain D consists of residues 39-182. A moiety well fit by an acetate molecule was found within chain D, consistent with the presence of acetate in the crystallization buffer. This acetate molecule was coordinated by a water molecule and is not expected to be functionally relevant.

Strain and plasmid constructions for complementation assays

Bacterial strains and plasmids used are listed in Table S1. Knockout strains (WT and *ΔcusS*) were made using the lambda-Red-mediated gene recombination technique as described by Datsenko and Wanner[12]. Briefly, the *cat* gene was PCR amplified with FRT sites from the pKD3 plasmid, using primers containing the flanking regions corresponding to the gene to be deleted from the genome. The temperature sensitive pCP20 plasmid encoding the FLP recombinase was used to remove the antibiotic resistance cassettes in the *ΔcusS* strain, the *cat* cassette was not removed from the WT strain. For growth experiments, the WT strain was transformed with pET21b(+) empty vector and the *ΔcusS* strain was transformed with each of the eight plasmids listed in Table S1.

To create the plasmid constructs expressing wild-type and mutant versions of full-length CusS, the *cusS* gene was PCR amplified and cloned into the multiple cloning site of pET21b(+) using the restriction enzymes NheI and XhoI. The resulting construct containing the full length *cusS* gene (*pcusS*) was used as a template for mutagenesis using the QuikChange Kit. Constructs were made with mutations of the metal binding residues at the interface binding site H42A/F43I/H176A (*pcusS-AIA*), the internal binding sites M133I/M135I/H145A (*pcusS-IIA*), and in both the interface and internal binding sites H42A/F43I/H176A/M133I/M135I/H145A (*pcusS-AIA-IIA*). Single mutations were also made of the metal binding residues at the interface binding site (*pcusS-H42A*, *pcusS-F43I*, *pcusS-H176A*). All plasmids were purified and sequenced for accuracy.

In vivo complementation assays on $CuSO_4$-containing plates

All strains containing the necessary plasmids were grown in Luria Broth (LB) media containing 100 μg/mL ampicillin at 37°C overnight. Fresh LB media containing 100 μg/mL was inoculated with the overnight cultures by 1:50 dilution, then growth was continued at 37°C for 3.5 hr. Cell densities were normalized to OD_{600} of 0.8 with LB containing 100 μg/mL ampicillin. Serial dilutions from 1 to 10^{-7} were made from this culture. All dilutions were spotted twice onto LB agar plates containing 100 μg/mL ampicillin, 1 mM IPTG, and a range of $CuSO_4$ concentrations (0–3 mM). Plates were incubated at 37°C for 24 hr, then cell growth was scored on a scale of 0–8, with 8 representing cells that grew in the last dilution (10^{-7}) and 0 representing no cell growth. The scores were converted to % cell survival, with 100% survival representing cell growth out to 10^{-6} and 10^{-7} dilutions. Conversion between scores and % cell survival is shown in Table S2. All growth experiments were conducted a minimum of three times.

Determination of intracellular copper accumulation in $CuSO_4$-containing media

To determine the copper accumulation in cells, all nine strains used in the *in vivo* complementation assays were grown in LB media as described above. When cells reached an OD_{600} = 0.8–0.9, cells were given 1 mM IPTG and 0.5 mM $CuSO_4$, and growth was

continued at 37°C. Cell aliquots were collected before induction as 0 hr samples, and then aliquots were collected at 3 and 6 hrs after addition of IPTG and $CuSO_4$. All cultures were normalized to a final OD_{600} of 0.8 and centrifuged to obtain cell pellets. The cell pellets were washed three times with sterile 1X PBS containing 1 mM EDTA to remove excess extracellular copper. Washed pellets were dried at 75°C for 2 hr in Savant SPD1010 SpeedVac Concentrator (Thermo Scientific). To each pellet, 1 mL of 70% trace metals nitric acid was added and cells were mineralized at 80°C for 2 hr. Samples were then diluted to a final nitric acid concentration of 4% with nano-pure water. Samples were analyzed in a graphite furnace iCE3400 atomic absorption spectrometer (Thermo Scientific). A standard calibration curve was generated using 0 to 40 ppb Cu, with final $R^2 \geq 0.99$. The concentration of copper for each strain was determined as an average of four replicates. Statistical significance of the data was determined using t-test analysis.

RESULTS

Overall structure of Ag(I)-$CusS_{(39\text{-}187)}$

The overall structure of Ag(I)-$CusS_{(39\text{-}187)}$ is a mixed α/β fold with a PAS-like topology (Figure 1). The central five-stranded anti-parallel β-sheet is flanked by α-helices on either side. This fold differs from the common PAS fold[13] in that the structure begins with a long N-terminal α-helix and ends with a short C-terminal α-helix that both lie on the same side of the sheet. This topology has been identified in the structures of other histidine kinase sensor domains such as PhoQ (PDB ID: 3BQ8), DcuS (PDB ID: 3BY8), and CitA (PDB ID: 2J80), which were the initial three α/β fold sensor domains whose structures were solved[14–16]. Thus this fold has been termed the PDC (PhoQ-DcuS-CitA) fold[13]. The long N-terminal helix is expected to continue into transmembrane helix 1 (identified as residues 15-37 from TMHMM v. 2.0[10]) and the short C-terminal helix would be followed by transmembrane helix 2 (identified as residues 187-206 from TMHMM v. 2.0) in the full-length protein.

There are four Ag(I)-$CusS_{(39\text{-}187)}$ molecules in the asymmetric unit that interact to form two homodimers, similar to the homodimers seen in other sensor domains of two-component systems as discussed below. The two homodimers in the asymmetric unit have similar structures, as determined by pairwise superposition using Superpose v. 1.0[17]. The overall root-mean-square deviation (r.m.s.d.) for the C^{α} atoms was calculated to be 0.588 Å with the greatest deviations in the loop regions. The B-factors in the two dimers are also similar to each other throughout the structure. The highest B-factors are observed in the loops (residues 64-68, 130-146, 156-164), suggesting flexibility in these regions.

The contacts between the two subunits of the homodimer are primarily between their N- and C-terminal helices, which form a central parallel helical bundle (Figure 2). PDBePISA (Proteins, Interfaces, Structures, and Assemblies) was used to calculate the buried surface area and complex formation significance score (CSS)[18]. The buried surface area was calculated to be 1720 $Å^2$ between chains A and B, and 1470 $Å^2$ between chains C and D. In this algorithm, the CSS values range from 0 to 1 as interface relevance to complex formation increases. The CSS value was determined to be 0.387 for both homodimers in the asymmetric unit. This relatively low value indicates that the interface has little relevance to

formation of the homodimer complex, however, this calculation did not take into consideration the metal ion binding sites that are at the dimer interface.

Structural similarities of Ag(I)-CusS$_{(39-187)}$ to other proteins

The structure of Ag(I)-CusS$_{(39-187)}$ was submitted to the DALI server v. 3 to identify other proteins in the Protein Data Bank (PDB) that have similar 3D structures[19]. The top six similar structures that were identified are the sensor domains of histidine kinases of other two-component systems: WalK (PDB ID: 4YWZ[20]), ResE (PDB ID: 4ZR7, unpublished), CdgS9 (PDB ID: 4U65 [21], CitA (PDB ID: 2J80[16]), TlpB (PDB ID: 3UB8[22]), and PhoQ (PDB ID: 3BQ8[14]), with Z-scores of 10.1, 9.4, 8.3, 7.8, 7.5, and 7.5 respectively. The backbone r.m.s.d.'s of these structures compared to Chain A of Ag(I)-CusS$_{(39-187)}$ are 2.5, 2.8 Å, 3.1 Å, 3.3 Å, 3.8 Å, and 3.4 Å respectively. WalK is a histidine kinase involved in regulating cell wall homeostasis; ResE is a histidine kinase involved in the regulation of aerobic and anaerobic respiration; LapD ortholog CdgS9 is involved in the regulation of biofilm formation; CitA is a histidine kinase that regulates the transport and anaerobic metabolism of citrate; TlpB is a pH sensing histidine kinase; PhoQ is a Mg^{2+} sensing histidine kinase involved in the regulation of virulence and stress response[14, 16, 21–24]. These sensor domains, like Ag(I)-CusS$_{(39-187)}$, have the same PDC fold with a central five-stranded antiparallel β-sheet flanked by α-helices. None of these proteins has significant sequence homology to CusS$_{(39-187)}$ (identity scores range from 9–17%).

Metal binding sites

Despite the similar folds of Ag(I)-CusS$_{(39-187)}$ and other sensor domains of two-component systems, these other sensor domains respond to widely different stimuli. No other structures of sensor domains that respond to Cu(I) or Ag(I) have been determined, and therefore the Ag(I)-CusS$_{(39-187)}$ structure provides a unique opportunity to understand responsiveness to these monovalent metal ions.

Eight silver ions were observed in the asymmetric unit, with four of the Ag(I) ions associated with each homodimer (Figure 2). In each dimer, two of the Ag(I) ions (Ag1 and Ag2) are symmetrically located at the dimer interface ("interface" binding sites), and the other two Ag(I) ions (Ag3 and Ag4) are in the outer loops of each monomer ("internal" binding sites) (Figure 3). The internal binding sites are approximately 17 Å away from the interface binding sites. The residues that coordinate the metal ions at the dimer interface are contributed from both subunits of the dimer: Ag1 is coordinated with the sidechains of F43 from α1 and H176 from α4 of chain A, and H42′ from α1′ of chain B. Ag2 interacts with the sidechains of H42 from α1 of chain A, and F43′ from α1′ and H176′ from α4′ of chain B. The internal binding site residues are contained within each subunit of the dimer: Ag3 in subunit A is coordinated by the sidechains of M133, M135, H145, and the carboxylic oxygen from the backbone of S84, and Ag4 is similarly coordinated in the other monomer. Strong electron density for each of these Ag(I) ions is consistent with full occupancy of the Ag(I) site (Figure S1).

The metal coordination site at the dimer interface is unusual in that a phenylalanine residue coordinates with the Ag(I) ion. A search of the PDB using Ligand Expo[25] for entries

containing Ag(I) resulted in 17 entries for different proteins. The only protein that interacts with Ag(I) using an aromatic ring is Ag(I)-CusF (PDB ID: 2QCP and 2VB3), which has a Ag(I)-W44 interaction[26, 27], though no structures show phenyl-Ag(I) interactions. In Ag(I)-$CusS_{(39-187)}$, the benzene ring of F43 is located above the Ag(I) ion and is slightly tilted, forming a cation-π interaction with the Ag(I) ion. The average bond lengths from the Ag(I) ions to the coordinating sidechain atoms are given in Table 2. The distances between the Ag(I) ions and the histidine nitrogens are approximately 2.20 Å, while the center of the F43 phenyl ring is at a distance of 3.30 Å from the Ag(I) ion. This site shows a nearly linear N-Ag-N geometry with the Ag(I) ion slightly displaced towards the benzene ring.

The internal Ag(I) binding sites in $CusS_{(39-187)}$ are formed by residues from loop regions of one monomer. These four-coordinate sites are formed by two methionines and one histidine, as well as the carbonyl oxygen from the backbone of a serine residue. Histidine and methionine ligands are commonly used for Cu(I)/Ag(I) coordination in oxidizing environments like the periplasm where the CusS sensor domain is located[28, 29]. The distances between Ag(I) and the methionines sulfurs are approximately 2.5 Å (Table 2).

Sequence comparisons of $CusS_{(39-187)}$ homologs and other Cu(I)/Ag(I) binding proteins

The sequence of *E. coli* K12 CusS was used as a query for BLAST analysis. The results of this inquiry showed that the full length histidine kinase CusS is prevalent in the Proteobacteria phylum, more specifically Gammaproteobacteria[30]. Homologs with high scores and high query coverage were also found in Betaproteobacteria, but not in Alpha, Delta, Epsilon, or Zetaproteobacteria. When the Proteobacteria phylum was excluded during the BLAST analysis to identify other homologous proteins in other bacterial phyla, two other hits with high query coverage were found: one is an ATPase from *Opitutaceae bacterium* (Verrucomicrobia phylum) and the other is a sensor histidine kinase from *Streptococcus pneumoniae* (Gram-positive Firmicutes phylum). Figure 4 shows the multiple-sequence alignment of the N-terminal portion (including the sensor domains) of these protein homologs to *E. coli* CusS, which was performed using T-coffee and edited by BoxShade (v. 3.21)[31]. Though SilS, CopS, and CinS were not identified from the BLAST results, they were also included in the multiple sequence alignments because they have been identified as putative metal-sensing histidine kinases[32–34]. The alignments show that H42, F43, and H176 from the interface binding site are conserved in all sequences, while M133, M135, and H145 from the internal binding site are not.

Functional roles of the metal binding sites in CusS

To investigate the role of metal binding sites in metal resistance by CusS *in vivo*, *E. coli* cells expressing full length CusS wild type and mutant constructs were evaluated for survival on $CuSO_4$-containing media (Figure 5). Growth experiments were performed in an *E. coli* strain (WT) in which the chromosomal copy of the gene for the multicopper oxidase CueO has been deleted (*ΔcueO).* CueO converts Cu(I) to Cu(II) and therefore the use of the strain with the *cueO* deletion allows the observation of a growth phenotype even under aerobic conditions[35]. The chromosomal copy of *cusS* was deleted from this background strain to allow characterization of CusS variants expressed from a plasmid. The WT strain was transformed with pET21b(+) empty vector, and *ΔcusS* strains were transformed with

pET21b(+) empty vector, plasmids containing full length *cusS* wild type (*pcusS*), or *cusS* mutant constructs (Table S1). Metal ligands in each binding site were altered from His to Ala, Phe to Ile, and Met to Ile. One variant eliminated the interface metal ion binding residues (H42A/F43I/H176A, *pcusS-AIA*), and another eliminated the internal binding site (M133I/M135I/H145A, *pcusS-IIA*). A variant in which all metal ion binding sites were altered was also tested (H42A/F43I/H176A/M133I/M135I/H145A, *pcusS-AIA-IIA*). Single mutations of the residues at the interface metal binding site (*pcusS-H42A*, *pcusS-F43I*, *pcusS-H176A*) were also made and transformed into *ΔcusS* strains.

As shown in Figure 5, the WT strain experiences copper susceptibility at 2.75 mM $CuSO_4$, whereas *ΔcusS* cells show a phenotype at lower concentrations. The *ΔcusS* cells have a decreased percentage of cell survival after 1.25 mM $CuSO_4$ and show no growth after 2 mM $CuSO_4$. The growth defects observed in the *ΔcusS* strain can be partially rescued by expression of intact CusS from a plasmid *(ΔcusS/pcusS)*. Although it is not a full phenotype complementation, the % cell survival is significantly higher than *ΔcusS* and growth is observed up to 2.5 mM $CuSO_4$. When the interface binding sites are mutated (*ΔcusS*/*pcusS-AIA*), the cell growth is altered at 1.25 mM $CuSO_4$ and no growth is seen past 1.75 mM $CuSO_4$. When the internal binding sites are mutated (*ΔcusS*/*pcusS-IIA*), the cells containing this construct show similar growth to the cells with intact CusS (*ΔcusS/pcusS)*. When all the metal binding residues from both the interface and internal binding sites are mutated, the cells containing this construct show altered growth at 1.25 mM $CuSO_4$. Growth of cells containing the construct in which both metal sites are deleted is not significantly different than those cells with the construct in which only the interface metal site has been deleted.

The residues in the interface binding sites were individually mutated to test their contribution to copper resistance. The *ΔcusS* strain was transformed with *pcusS-H42A*, *pcusS-F43I*, or *pcusS-H176A* plasmids. As shown in Figure 5, the H42A and H176A alterations (*ΔcusS/pcusS-H42A* and *ΔcusS/pcusS-H176A* respectively) result in the same growth defects as the construct in which all interface binding site residues are mutated. The cells expressing the construct with the F43I alteration (*ΔcusS/pcusS-F43I)* have a slightly higher % cell survival compared to *ΔcusS/pcusS-H42A*, *ΔcusS/pcusS-H176A* or *ΔcusS/pcusS- AIA*.

To ensure that the full length CusS wild type and mutant proteins were expressed at the similar level from the pET21b(+) plasmids, Western blot analysis was performed. The expression of CusS proteins were detected with an anti-6xHis tag antibody. The expression level of each CusS wild type and mutants was similar, and no expression of CusS protein was detected from the WT and *ΔcusS* with pET21b empty vector (Figure S2). The mutations do not significantly affect the relative expression levels of CusS.

Effects of CusS metal ion binding site variants on copper accumulation in *E. coli*

To study the effects of CusS variants on copper accumulation, intracellular copper concentrations of cells stressed with $CuSO_4$ were measured. Cell strains as described in the previous section were grown aerobically in copper-containing media. Time point samples were collected at 0, 3, and 6 hr, and copper levels were measured by GFAAS. As shown in Figure 6, the *ΔcusS* strain had a significant increase in copper accumulation with a five-fold

increase compared to the WT strain after 3 hr, and with an 11-fold increase after 6 hr. Providing *cusS* on a plasmid (*ΔcusS/pcusS*) rescued the phenotype, decreasing copper concentrations from 58 ng Cu/10^9 cells to 41 ng Cu/10^9 cells after 3 hr and from 60 ng Cu/10^9 cells to 34 ng Cu/10^9 cell after 6 hr. When the cells were transformed with *cusS* containing the different mutations disrupting either interface or internal binding sites (*ΔcusS/pcusS-AIA* and *ΔcusS/pcusS-IIA* respectively), or both interface and internal binding sites (*ΔcusS/pcusS-AIA-IIA*), the intracellular copper concentrations increase significantly compared to the WT and *ΔcusS/pcusS* strains. Individual mutations of the residues forming the interface binding site *(ΔcusS/pcusS-H42A*, *ΔcusS/pcusS-H176A*, and *ΔcusS/pcusS-F43I)* also result in similar accumulations of copper inside the cells.

DISCUSSION

Ag(I)-$CusS_{(39\text{-}187)}$ is a homodimer with four Ag(I) binding sites. Each monomer has the PAS-like PDC fold, in which α-helical elements lie on both sides of a central antiparallel β sheet. $CusS_{(39\text{-}187)}$ is structurally similar to a number of other sensing domains of histidine kinases, despite overall low sequence identities. The sequence diversity of the different sensor domains allows for detection of widely varying stimuli in the environment. However, it may be that the use of similar overall folds of the sensor domains allows a common mechanism of activation of the conserved kinase core upon stimulus, as discussed below.

Despite having a similar overall fold to some sensor domains of histidine kinases from other systems, $CusS_{(39\text{-}187)}$ binds its ligand in a unique position within this structure. As shown in Figure 7, other PDC-fold sensor domains, such as CitA, TlpB, and DcuS[15, 16, 22], have binding sites located in the outer loop area. While $CusS_{(39\text{-}187)}$ has a binding site in the outer loop (the internal binding site), it also has binding site formed by residues in the N- and C-terminal helices (the interface binding site). Of these two sites, based on sequence conservation (Figure 4) and effects of mutations on ability to survive on copper-containing media (Figure 5), the interface metal ion binding site is more functionally important than the internal metal ion binding site. The affinities of CusS for metal ions at each binding site are not known, but it may be that the interface binding site arose because it allowed response at more biologically appropriate levels of metal ions, while the internal binding site has remained as an evolutionary relic. Future experiments that determine affinities and selectivities for metal ions may support or refute this idea.

The interface metal ion binding site of $CusS_{(39\text{-}187)}$ uses a novel set of ligands to coordinate the silver ion as compared to other Ag(I)-binding proteins. The Ag(I) ions in the interface binding sites are coordinated by two His from each subunit in an approximately linear geometry, with a Phe residue forming a cation-π interaction. The His-Ag(I) bonds lengths are similar to those previously reported for Ag(I) bound to small molecules or proteins[26, 28, 36–38]. While there are now examples of proteins and small molecules that coordinate Ag(I) or Cu(I) with the indole ring of Trp[26, 27, 39], this is the first example of a biological system where a protein's phenyl ring forms a cation-π interaction with Ag(I). Small molecule-Ag(I) complexes generally have distances of 2.4–2.6 Å between the ring center and the silver ion for cation-π interactions, which is shorter than the 3.3 Å distance observed in Ag(I)-$CusS_{(39\text{-}187)}$. The cation-π interaction in Ag(I)-$CusS_{(39\text{-}187)}$ is also

slightly longer than the Ag(I)-Trp cation-π interaction in CusF (distances between the Ag(I) ion and the CE3 and CZ3 of W44 in CusF are 2.82 Å and 2.96 Å, respectively)[26]. However, significant cation-π interactions may be found at distances up to 6 Å[40]. Though the Ag(I)-Phe interaction in CusS is long, it is clearly functionally significant, as the F43I mutation significantly affects the ability of *E. coli* to survive on copper-containing media (Figure 5). The His_2Phe coordination is likely to be very selective for Ag(I) and Cu(I), and therefore will help to provide specificity for the resistance system. In other systems, it has been shown that cation-π interactions are likely to be important for selectivity and transport of Na^+ and K^+ across membranes[41]. In CusS, the interaction of Cu(I) and the aromatic ring via π-electrons may play a role in protecting Cu(I) against oxidation, and thereby contribute to protection of the periplasm from copper toxicity[26, 39].

Previous studies of $CusS_{(39\text{-}187)}$ in solution found that 4 Ag(I) ions are bound per monomer,[11], though the crystal structure reported here shows two Ag(I) ions per $CusS_{(39\text{-}187)}$ monomer. This disparity may be due to differences in sample preparation, and may reflect the fact that Ag(I) can bind non-specifically to proteins. $CusS_{(39\text{-}187)}$ has numerous His and Met residues (9 and 7, respectively) of which several are clustered in the outer loop of the sensor domain. It is possible that Ag(I) ions are weakly bound by these residues in solution, and therefore are not reflected in the crystal structure.

The expression of CusS from a plasmid does not result in the same growth phenotype on copper-containing media as the strain that expresses chromosomal CusS. The expression of CusS from the chromosome in the presence of copper is much lower overall than the expression of CusS from a plasmid following IPTG induction (Figure S1). The stress of expressing relatively high levels of this 54 kDa membrane protein may be the reason that full complementation is not achieved from the plasmid-expressed CusS. Additionally, how much functional protein is expressed from the plasmid system is not known.

In response to periplasmic Ag(I) and Cu(I), CusS upregulates the genes to express the CusCBA Cu(I)/Ag(I) efflux pump to remove excess metal ions from the cell. Previous studies have shown that loss of the *cusS* gene results in an increase in intracellular copper levels, likely due to lack of upregulation of *cusCFBA* resulting in decreased metal ion export[9]. Here, we have further investigated the specific effects on copper accumulation when the metal ion binding site residues in CusS are altered. The results (Figure 6) suggest that direct metal ion binding by the sensor domain is key to triggering the copper resistance response. Single mutations of the interface metal ion binding site residues have similar effects to the mutation of all three residues simultaneously. The copper accumulation of cells with mutations in the internal metal ion binding site is not significantly different from the cells with mutations to the interface binding residues. This may be due to the fact that the accumulation studies were performed at a level of copper (0.5 mM) where no growth defects are observed for any of the constructs tested (Figure 5). Since increases in copper accumulation occur in the cells where single residues from the interface binding sites were mutated, this shows that all residues contribute to the downstream activation of *cusCFBA*.

Histidine kinases function as dimers and signal transduction processes occurs through the dimeric interface[5]. However, many sensor domains of histidine kinases, such as DcuS, DctB,

CitA, and NarX, are monomeric in solution[15, 16, 42]. Analytical ultracentrifugation and *in vitro* crosslinking experiments have demonstrated that apo-$CusS_{(39-187)}$ is primarily monomeric in solution, though $CusS_{(39-187)}$ dimerization is enhanced by the addition of Ag(I)[11]. Ligand binding has also been observed to induce dimerization of the sensor domains of the histidine kinases NarX and CitA, which bind nitrate and citrate, respectively[16, 42]. Based on CSS calculations of the Ag(I)-$CusS_{(39-187)}$ crystal structure, the dimer interface has low relevance to complex formation. However, this calculation does not take into account the Ag(I) ions at the interface and the presence of Ag(I) is likely to strengthen the dimeric interface.. Taking the above information into account, the Ag(I)-$CusS_{(39-187)}$) dimer observed in the crystal structure is likely to be the predominant form of the sensor domain in the presence of the ligand.

How ligand binding in the sensor domain leads to activation of the cytoplasmic kinase function remains an open question. Dimerization of the sensor domain of CitA upon binding to citrate is hypothesized to trigger piston-like movement at the dimeric interface, and thus transduce signal to the cytoplasmic side to activate the kinase core[16]. In the PDC-fold sensor domains of canonical histidine kinases, the N- and C-terminal helices are expected to be contiguous with the transmembrane helices. Thus conformational changes in these helices in the periplasm could be propagated into the cytoplasmic portion of the kinase and provide a direct mechanism for altering kinase activity. In the CusS sensor domain structure described here, the interface metal ion binding site is well-positioned to result in this kind of structural change that could lead to activation. However, more studies are needed to determine the conformational differences between the apo and metal ion-bound states and how these precisely lead to activation.

Supplementary Material

Refer to Web version on PubMed Central for supplementary material.

Acknowledgments

Funding Sources

This manuscript is based on work supported by National Institutes of Health grant GM079192.

The authors acknowledge the Stanford Synchrotron Radiation Lightsource where diffraction data were collected. We thank Dr. Sue A. Roberts for her assistance with X-ray data collection.

ABBREVIATIONS

E. coli	Escherichia coli
HAMP	Histidine kinases, adenylyl cyclases, methyl-accepting proteins, phosphatases
DHp	Dimerization and histidine phosphotransfer
SAD	Single anomalous diffraction
LB	Luria Broth

GFAAS Graphite furnace atomic absorption spectrometer

References

1. Rensing C, Grass G. Escherichia coli mechanisms of copper homeostasis in a changing environment. FEMS Microbiol Rev. 2003; 27:197–213. [PubMed: 12829268]
2. Beswick PH, Hall GH, Hook AJ, Little K, McBrien DC, Lott KA. Copper toxicity: evidence for the conversion of cupric to cuprous copper in vivo under anaerobic conditions. Chem Biol Interact. 1976; 14:347–356. [PubMed: 182394]
3. Outten FW, Huffman DL, Hale JA, O'Halloran TV. The independent cue and cus systems confer copper tolerance during aerobic and anaerobic growth in Escherichia coli. J Biol Chem. 2001; 276:30670–30677. [PubMed: 11399769]
4. Franke S, Grass G, Nies DH. The product of the ybdE gene of the Escherichia coli chromosome is involved in detoxification of silver ions. Microbiology. 2001; 147:965–972. [PubMed: 11283292]
5. Stock AM, Robinson VL, Goudreau PN. Two-component signal transduction. Annu Rev Biochem. 2000; 69:183–215. [PubMed: 10966457]
6. Yamamoto K, Hirao K, Oshima T, Aiba H, Utsumi R, Ishihama A. Functional characterization in vitro of all two-component signal transduction systems from Escherichia coli. J Biol Chem. 2005; 280:1448–1456. [PubMed: 15522865]
7. Gordeliy VI, Labahn J, Moukhametzianov R, Efremov R, Granzin J, Schlesinger R, Buldt G, Savopol T, Scheidig AJ, Klare JP, Engelhard M. Molecular basis of transmembrane signalling by sensory rhodopsin II-transducer complex. Nature. 2002; 419:484–487. [PubMed: 12368857]
8. West AH, Stock AM. Histidine kinases and response regulator proteins in two-component signaling systems. Trends Biochem Sci. 2001; 26:369–376. [PubMed: 11406410]
9. Gudipaty SA, Larsen AS, Rensing C, McEvoy MM. Regulation of Cu(I)/Ag(I) efflux genes in Escherichia coli by the sensor kinase CusS. FEMS Microbiol Lett. 2012; 330:30–37. [PubMed: 22348296]
10. Krogh A, Larsson B, von Heijne G, Sonnhammer EL. Predicting transmembrane protein topology with a hidden Markov model: application to complete genomes. J Mol Biol. 2001; 305:567–580. [PubMed: 11152613]
11. Gudipaty SA, McEvoy MM. The histidine kinase CusS senses silver ions through direct binding by its sensor domain. Biochim Biophys Acta. 2014; 1844:1656–1661. [PubMed: 24948475]
12. Datsenko KA, Wanner BL. One-step inactivation of chromosomal genes in Escherichia coli K-12 using PCR products. Proc Natl Acad Sci U S A. 2000; 97:6640–6645. [PubMed: 10829079]
13. Cheung J, Hendrickson WA. Sensor domains of two-component regulatory systems. Curr Opin Microbiol. 2010; 13:116–123. [PubMed: 20223701]
14. Cheung J, Bingman CA, Reyngold M, Hendrickson WA, Waldburger CD. Crystal structure of a functional dimer of the PhoQ sensor domain. J Biol Chem. 2008; 283:13762–13770. [PubMed: 18348979]
15. Cheung J, Hendrickson WA. Crystal structures of C4-dicarboxylate ligand complexes with sensor domains of histidine kinases DcuS and DctB. J Biol Chem. 2008; 283:30256–30265. [PubMed: 18701447]
16. Sevvana M, Vijayan V, Zweckstetter M, Reinelt S, Madden DR, Herbst-Irmer R, Sheldrick GM, Bott M, Griesinger C, Becker S. A ligand-induced switch in the periplasmic domain of sensor histidine kinase CitA. J Mol Biol. 2008; 377:512–523. [PubMed: 18258261]
17. Maiti R, Van Domselaar GH, Zhang H, Wishart DS. SuperPose: a simple server for sophisticated structural superposition. Nucleic Acids Res. 2004; 32:W590–594. [PubMed: 15215457]
18. Krissinel E, Henrick K. Inference of macromolecular assemblies from crystalline state. J Mol Biol. 2007; 372:774–797. [PubMed: 17681537]
19. Holm L, Rosenstrom P. Dali server: conservation mapping in 3D. Nucleic Acids Res. 2010; 38:W545–549. [PubMed: 20457744]
20. Ji Q, Chen PJ, Qin G, Deng X, Hao Z, Wawrzak Z, Yeo WS, Quang JW, Cho H, Luo GZ, Weng X, You Q, Luan CH, Yang X, Bae T, Yu K, Jiang H, He C. Structure and mechanism of the essential

two-component signal-transduction system WalKR in Staphylococcus aureus. Nat Commun. 2016; 7:11000. [PubMed: 26987594]

21. Chatterjee D, Cooley RB, Boyd CD, Mehl RA, O'Toole GA, Sondermann H. Mechanistic insight into the conserved allosteric regulation of periplasmic proteolysis by the signaling molecule cyclic-di-GMP. Elife. 2014; 3:e03650. [PubMed: 25182848]
22. Goers Sweeney E, Henderson JN, Goers J, Wreden C, Hicks KG, Foster JK, Parthasarathy R, Remington SJ, Guillemin K. Structure and proposed mechanism for the pH-sensing Helicobacter pylori chemoreceptor TlpB. Structure. 2012; 20:1177–1188. [PubMed: 22705207]
23. Neiditch MB, Federle MJ, Pompeani AJ, Kelly RC, Swem DL, Jeffrey PD, Bassler BL, Hughson FM. Ligand-induced asymmetry in histidine sensor kinase complex regulates quorum sensing. Cell. 2006; 126:1095–1108. [PubMed: 16990134]
24. Baruah A, Lindsey B, Zhu Y, Nakano MM. Mutational analysis of the signal-sensing domain of ResE histidine kinase from Bacillus subtilis. J Bacteriol. 2004; 186:1694–1704. [PubMed: 14996800]
25. Feng Z, Chen L, Maddula H, Akcan O, Oughtred R, Berman HM, Westbrook J. Ligand Depot: a data warehouse for ligands bound to macromolecules. Bioinformatics. 2004; 20:2153–2155. [PubMed: 15059838]
26. Loftin IR, Franke S, Blackburn NJ, McEvoy MM. Unusual Cu(I)/Ag(I) coordination of Escherichia coli CusF as revealed by atomic resolution crystallography and X-ray absorption spectroscopy. Protein Sci. 2007; 16:2287–2293. [PubMed: 17893365]
27. Xue Y, Davis AV, Balakrishnan G, Stasser JP, Staehlin BM, Focia P, Spiro TG, Penner-Hahn JE, O'Halloran TV. Cu(I) recognition via cation-pi and methionine interactions in CusF. Nat Chem Biol. 2008; 4:107–109. [PubMed: 18157124]
28. Changela A, Chen K, Xue Y, Holschen J, Outten CE, O'Halloran TV, Mondragon A. Molecular basis of metal-ion selectivity and zeptomolar sensitivity by CueR. Science. 2003; 301:1383–1387. [PubMed: 12958362]
29. Peariso K, Huffman DL, Penner-Hahn JE, O'Halloran TV. The PcoC copper resistance protein coordinates Cu(I) via novel S-methionine interactions. J Am Chem Soc. 2003; 125:342–343. [PubMed: 12517140]
30. Altschul SF, Madden TL, Schaffer AA, Zhang J, Zhang Z, Miller W, Lipman DJ. Gapped BLAST and PSI-BLAST: a new generation of protein database search programs. Nucleic Acids Res. 1997; 25:3389–3402. [PubMed: 9254694]
31. Notredame C, Higgins DG, Heringa J. T-Coffee: A novel method for fast and accurate multiple sequence alignment. J Mol Biol. 2000; 302:205–217. [PubMed: 10964570]
32. Gupta A, Matsui K, Lo JF, Silver S. Molecular basis for resistance to silver cations in Salmonella. Nat Med. 1999; 5:183–188. [PubMed: 9930866]
33. Mills SD, Jasalavich CA, Cooksey DA. A two-component regulatory system required for copper-inducible expression of the copper resistance operon of Pseudomonas syringae. J Bacteriol. 1993; 175:1656–1664. [PubMed: 8449873]
34. Quaranta D, McEvoy MM, Rensing C. Site-directed mutagenesis identifies a molecular switch involved in copper sensing by the histidine kinase CinS in Pseudomonas putida KT2440. J Bacteriol. 2009; 191:5304–5311. [PubMed: 19542288]
35. Franke S, Grass G, Rensing C, Nies DH. Molecular analysis of the copper-transporting efflux system CusCFBA of Escherichia coli. J Bacteriol. 2003; 185:3804–3812. [PubMed: 12813074]
36. Davies H, Dilworth JR, Griffiths DV, Miller J, Zheng Y. The synthesis and crystal structures of the amide NS3 macrocycle L1, and the silver complexes [Ag(L1)]n[CF3SO3]n and of [Ag(L2)]2[CF3SO3]2(where L1=9-oxo-1,4,7-trithia-10-azacyclododecane andL2=7-oxo-2,5,11-trithia-8-azatetradecane-12-orthobenzenophane). Polyhedron. 1998; 18:459–467.
37. Chen CL, Su CY, Cai YP, Zhang HX, Xu AW, Kang BS, Zur Loye HC. Multidimensional frameworks assembled from silver(I) coordination polymers containing flexible bis(thioquinolyl) ligands: role of the intra- and intermolecular aromatic stacking interactions. Inorg Chem. 2003; 42:3738–3750. [PubMed: 12793810]

38. Gitschier J, Moffat B, Reilly D, Wood WI, Fairbrother WJ. Solution structure of the fourth metal-binding domain from the Menkes copper-transporting ATPase. Nat Struct Biol. 1998; 5:47–54. [PubMed: 9437429]

39. Okada M, Miura T. Copper(I) stabilization by cysteine/tryptophan motif in the extracellular domain of Ctr4. J Inorg Biochem. 2016; 159:45–49. [PubMed: 26908286]

40. Gallivan JP, Dougherty DA. Cation-pi interactions in structural biology. Proc Natl Acad Sci U S A. 1999; 96:9459–9464. [PubMed: 10449714]

41. Kumpf RA, Dougherty DA. A mechanism for ion selectivity in potassium channels: computational studies of cation-pi interactions. Science. 1993; 261:1708–1710. [PubMed: 8378771]

42. Cheung J, Hendrickson WA. Structural analysis of ligand stimulation of the histidine kinase NarX. Structure. 2009; 17:190–201. [PubMed: 19217390]

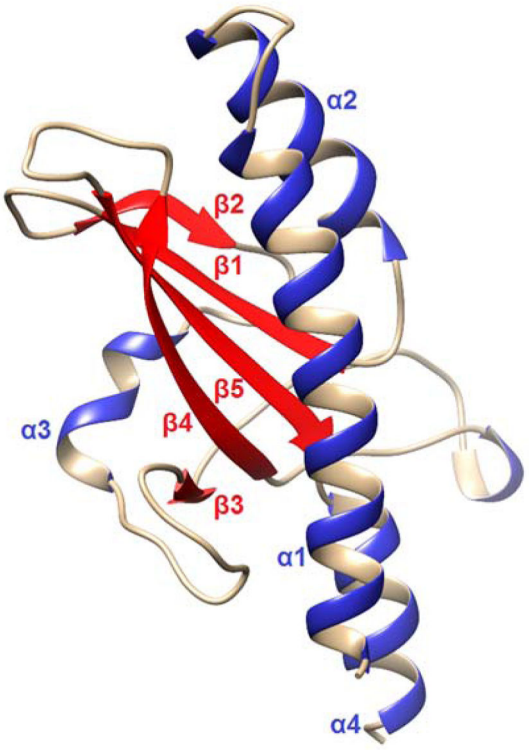

Figure 1.
Crystal structure of the Ag(I)-$CusS_{(39\text{-}187)}$ monomer.

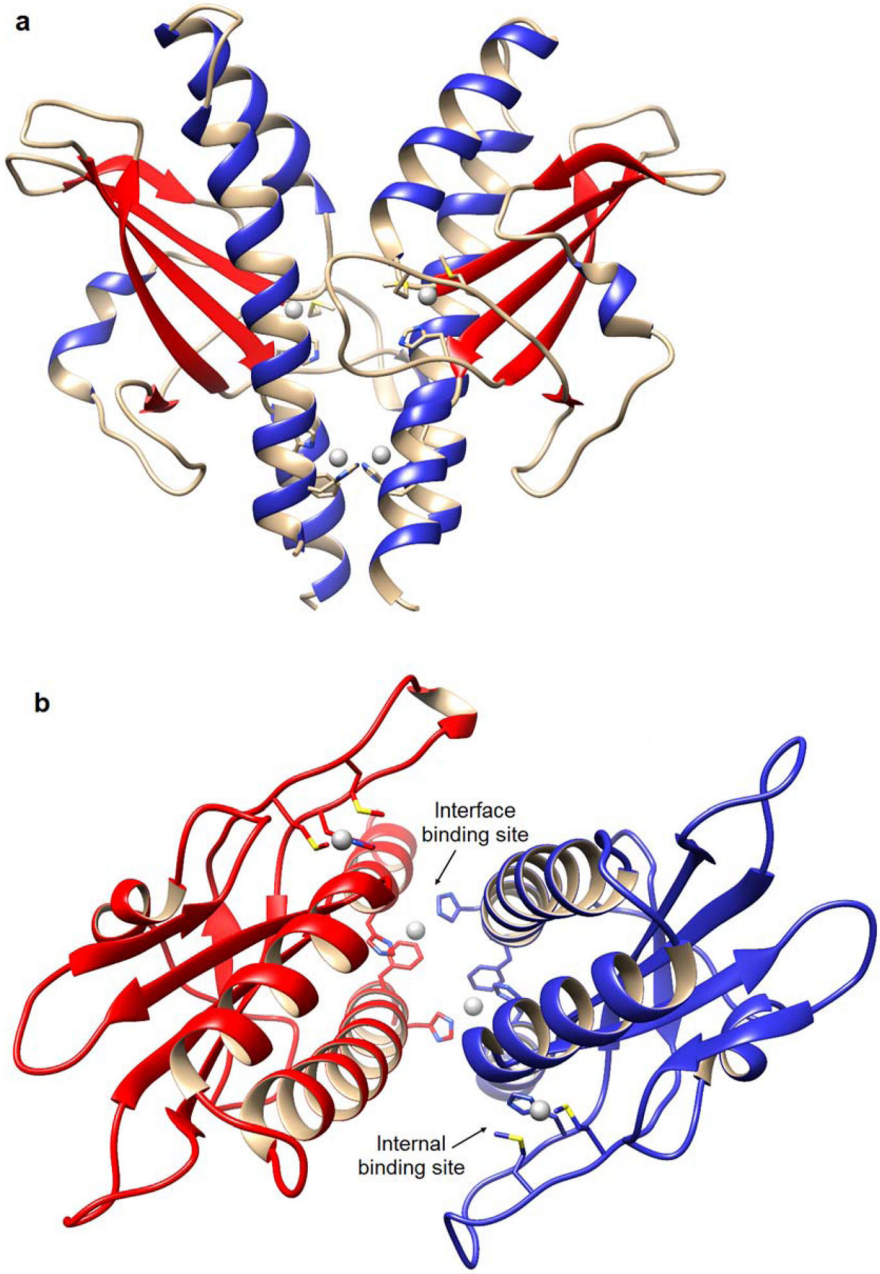

Figure 2.

Crystal structure of the Ag(I)-$CusS_{(39\text{-}187)}$ homodimer. (a) In this homodimeric structure of Ag(I)-$CusS_{(39\text{-}187)}$, the bound Ag(I) ions are shown as gray spheres and metal binding residues are shown in stick representation. (This view would be expected to be approximately perpendicular to the membrane for the intact protein *in vivo*.) (b) Top view (toward the membrane if looking at the protein *in vivo*) of the Ag(I)-$CusS_{(39\text{-}187)}$ homodimer highlighting the metal binding sites.

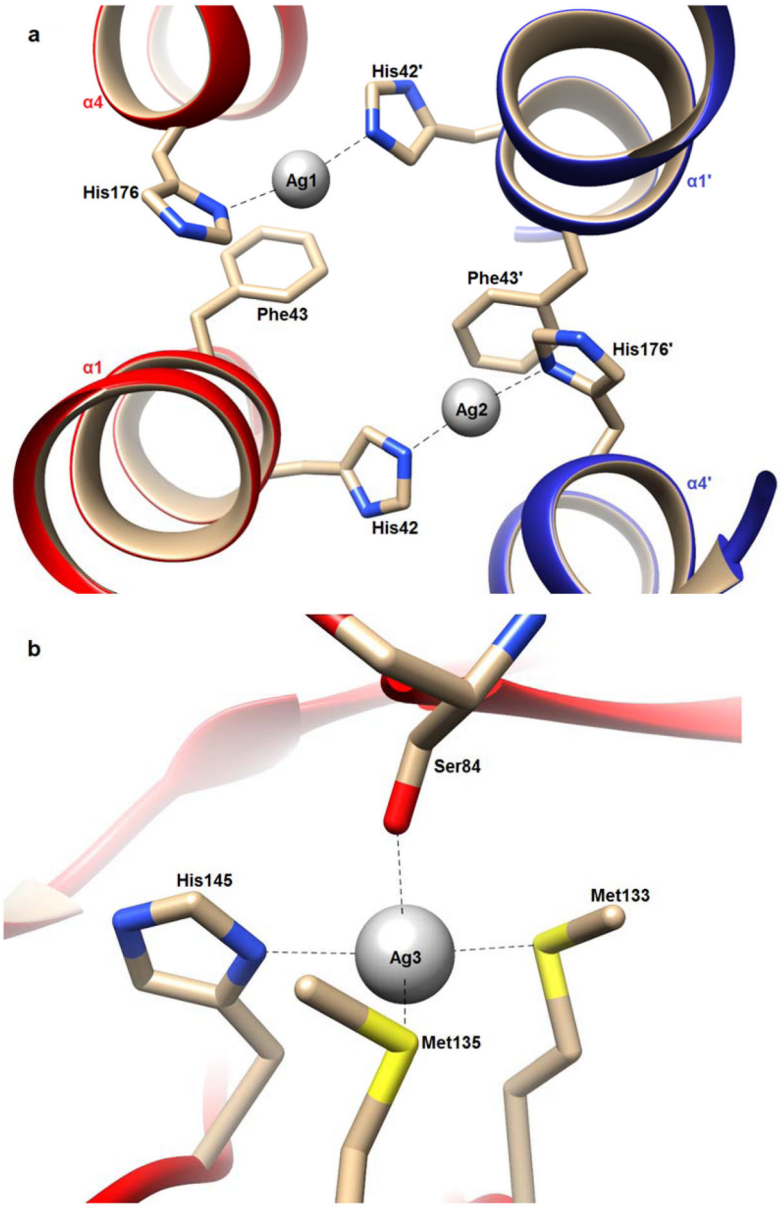

Figure 3.

Metal binding sites of Ag(I)-$CusS_{(39\text{-}187)}$. (a) Close-up view of the interface binding sites. (b) Close-up view of the internal binding site.

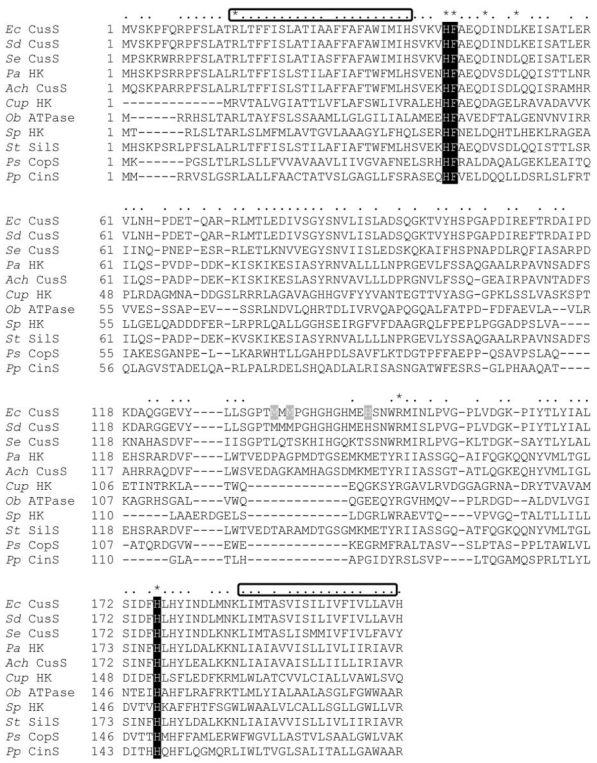

Figure 4.

Alignment of *Escherichia coli K12* CusS residues 1 to 207 with homologues from other organisms and other Cu(I)/Ag(I) sensing proteins. Highlighted in black and indicated with white text are the histidines and phenylalanine (H42, F43, and H176 from *E. coli W3110* CusS) in the interface binding site of $CusS_{(39\text{-}187)}$. Highlighted in dark gray and indicated with white text are the methionines and histidine (M133, M135, and H145 from E. coli W3110 CusS) that form the internal binding site. Conserved residues are labeled with asterisks. Horizontal black rectangles indicate the predicted transmembrane helices of *E. coli K12* CusS (predicted using the TMHMM server). Organism names are abbreviated in italics (*Ec* for *E. coli*, *Sd* for *Shigella dysenteriae*, *Se* for *Salmonella enterica*, *Pa* for *Pseudomonas aeruginosa*, *Ach* for *Achromobacter*, *Cup* for *Cupriavidus*, *Ob* for *Opitutaceae bacterium*, *Sp* for *Streptococcus pneumoniae*, *St* for *Salmonella typhimurium*, *Ps* for *Pseudomonas syringae*, and *Pp* for *Pseudomonas putida*). HK = histidine kinase

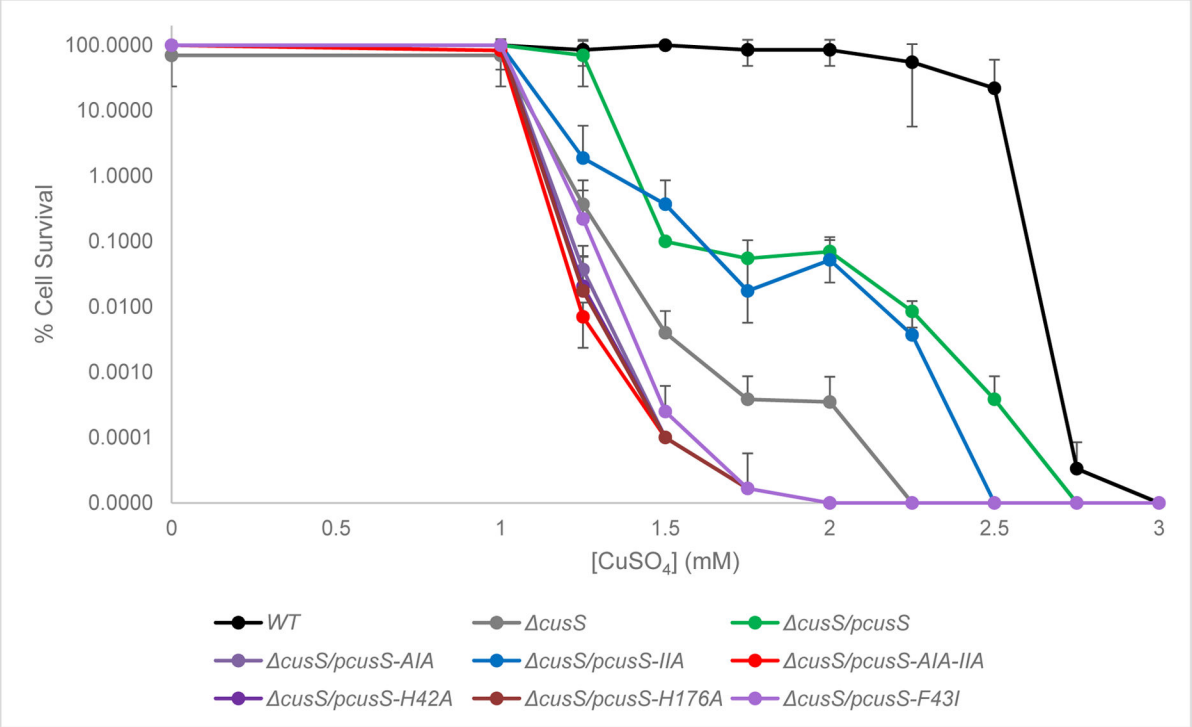

Figure 5.

Cell survival of BW25113*ΔcueOΔcusS* with pET21b-*cusS-WT/mutants* grown in various amounts of $CuSO_4$. Cells were grown at 37°C on LB agar plates supplemented with 100 μg/mL ampicillin, 1 mM IPTG, and various concentrations of $CuSO_4$ (0–3 mM) for 24 hr. The graph is shown relative to 100% cell survival, which is defined as cell growth in the 10^{-6} and 10^{-7} dilutions. Error bars indicate standard deviations of at least triplicate experiments.

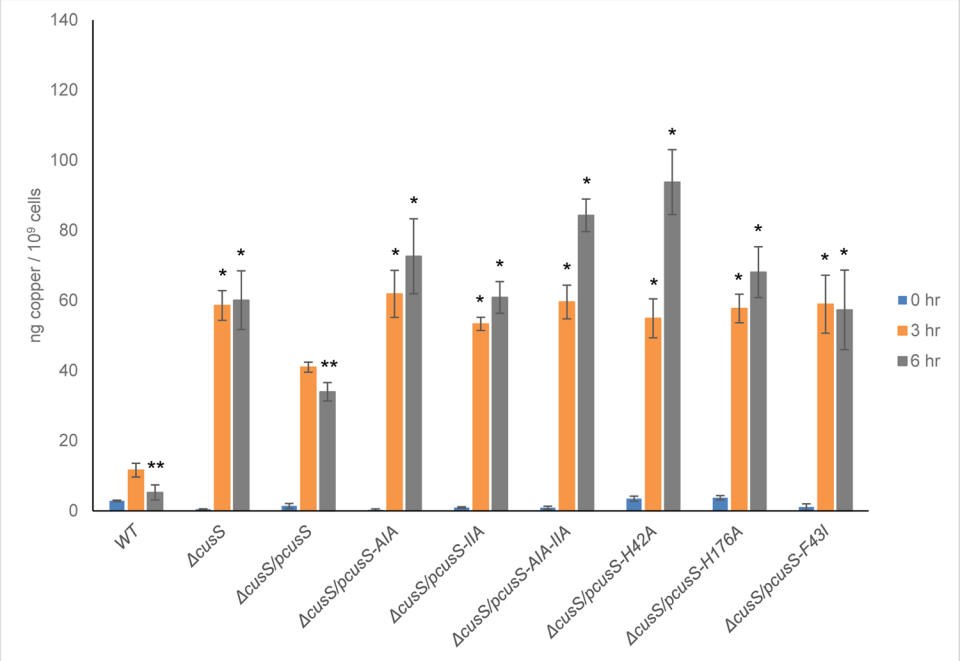

Figure 6.

Copper accumulation in *E. coli* cells grown in medium containing copper. The graph shows calculated copper accumulation in cell at 0 hr (blue), 3 hr (orange), and 6 hr (gray) after the addition of 0.5 mM $CuSO_4$. Copper levels are calculated as ng copper per 10^9 cells. Each bar represents the average of four replicates and the standard deviations are indicated by the error bars. * indicates a statistically significant difference from *ΔcusS/pcusS* with $P \leq 0.006$. ** indicates a statistically significant difference from 3 hr within the same cell strain with $P \leq 0.002$.

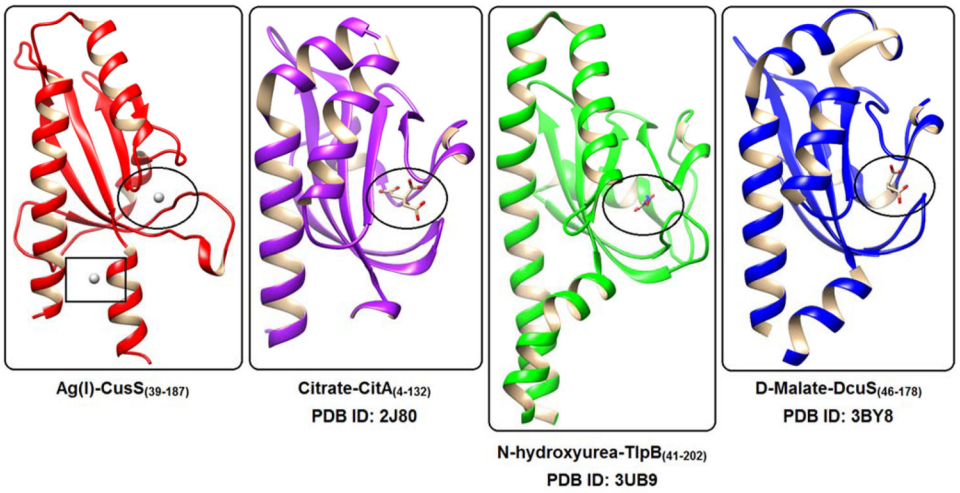

Figure 7.

Comparison of binding sites in sensor domains of CusS, CitA, TlpB, and DcuS. Structures of Ag(I)-$CusS_{(39-187)}$, citrate-$CitA_{(4-132)}$, N-hydroxyurea-$TlpB_{(41-202)}$, and D-malate-$DcuS_{(46-178)}$ are shown in red, purple, green, and blue respectively. Silver ions are shown as gray spheres and small molecules are shown in stick representation. Binding sites located in the outer loops are highlighted in ovals on all structures. The interface binding site of Ag(I)-$CusS_{(39-187)}$ is highlighted in a box.

Table 1

Data collection and refinement statistics

	Ag(I)-CusS$_{(39-187)}$	Ag(I)-CusS$_{(39-187)}$
Data Collection		
Wavelength (Å)	1.494	1.036
Space Group	P22121	P22121
Cell dimensions		
a, b, c (Å)	35.18, 95.71, 203.12	35.23, 96.29, 203.66
α, β, γ (°)	90, 90, 90	90, 90, 90
Resolution (Å)	35.18-2.80 (2.90-2.80)	33.29-2.15 (2.23-2.15)
Total reflections	468382	134231
Unique reflections	17836	38599
R_{merge} (%)	11.1 (29.5)	11.0 (40.9)
I/σ(I)	18.7 (9.5)	6.3 (2.4)
Completeness (%)	100.0 (100.0)	99.0 (99.8)
Redundancy	26.26 (26.85)	3.48 (3.52)
Refinement		
Resolution (Å)		2.15
R_{work}/R_{free}		24.97/28.64
No. of atoms		
Protein		4631
Ag		8
Acetate		4
Water		204
B factors		
Protein		34.9
Ag		27.3
Acetate		57.1
Water		32.7
R.m.s deviations		
Bond lengths (Å)		0.0063
Bond angles (°)		1.0596
Ramachandran plot (%)		
Most favored		97.73
Allowed		2.10
Outliers		0.17

Values in parentheses are for the highest-resolution shell.

R_{free} was calculated using 5% of the data set.

Table 2

Bond lengths in the metal ion binding sites of Ag(I)-$CusS_{(39\text{-}187)}$. Distances were measured for each monomer in the asymmetric unit, and the values shown are the averages of the four measurements, including the standard deviations.

Interface binding sites	**Bond lengths (Å)**
Ag-N3 (H42′)	2.18 ± 0.05
Ag-N1 (H176)	2.25 ± 0.06
Ag-Phenyl (F43)	3.30 ± 0.07
Internal binding sites	
Ag-S (M133)	2.45 ± 0.13
Ag-S (M135)	2.65 ± 0.06
Ag-N1 (H145)	2.05 ± 0.13
Ag-C=O (S84)	2.68 ± 0.10